Journal of ELECTRONIC MATERIALS, Vol. 46, No. 7, 2017
DOI: 10.1007/s11664-017-5445-5
© 2017 The Minerals, Metals & Materials Society

Fully Printed Memristors from Cu–SiO_2 Core–Shell Nanowire Composites

MATTHEW J. CATENACCI,[1] PATRICK F. FLOWERS,[1] CHANGYONG CAO,[2] JOSEPH B. ANDREWS,[2] AARON D. FRANKLIN,[1,2] and BENJAMIN J. WILEY[1,3]

1.—Department of Chemistry, Duke University, Durham, NC 27708, USA. 2.—Department of Electrical and Computer Engineering, Duke University, Durham, NC 27708, USA. 3.—e-mail: benjamin.wiley@duke.edu

This article describes a fully printed memory in which a composite of Cu–SiO_2 nanowires dispersed in ethylcellulose acts as a resistive switch between printed Cu and Au electrodes. A 16-cell crossbar array of these memristors was printed with an aerosol jet. The memristors exhibited moderate operating voltages (~3 V), no degradation over 10^4 switching cycles, write speeds of 3 μs, and extrapolated retention times of 10 years. The low operating voltage enabled the programming of a fully printed 4-bit memristor array with an Arduino. The excellent performance of these fully printed memristors could help enable the creation of fully printed RFID tags and sensors with integrated data storage.

Key words: Memristors, printed electronics, non-volatile memory, copper nanowires, nanowires

INTRODUCTION

Printed electronics enables the rapid prototyping of circuits on a wide variety of curved and flexible substrates, as well as the scalable and low-cost production of simple electronic components or devices.[1] Examples of printed electronic devices include circuit boards,[2] transistors,[3] sensors,[4] radio frequency identification (RFID) tags,[5] solar cells,[6] light-emitting diodes,[7] transparent electrodes,[8] touch screens,[9] amplifiers,[10] batteries,[11] flexible displays[12] and implantable bioelectronic devices.[13] An ongoing problem with printed electronics is the development of materials and processing methods that enable fully printed electronic components to have properties that are comparable to their silicon-based counterparts, or, at the very least, properties that are sufficient for practical use.

An area of printed electronics in which additional development is necessary is printable non-volatile memory, which will be essential for the development of fully printed RFID tags, e-paper, and sensors with integrated data storage.[14,15] One approach to creating a printed memory is by polarizing selected areas in a ferroelectric polymer film, such as those made from poly(vinylidene fluoride) (PVDF) and its copolymers with trifluoroethylene (TfFe).[16,17] Printed ferroelectric polymer memories have write speeds as short as 5 ms,[17] can be switched for as many as 10^3 cycles,[16] require high operating voltages (>15 V),[15] and exhibit short retention times (<1 h).[18] A second approach to creating a printed memory is the creation of a film that enables the trapping of charge in graphene oxide,[19] polymer,[20] or nanoparticle–polymer composites.[15] These devices can be operated at voltages as low as 1.5 V,[21] switch for up to 10^3 cycles,[22] have write speeds as fast as 10 ms,[20] and retain the charge for a few days. Kim et al.[19] reported a charge-trap-based memory that could retain an ON–OFF ratio of ~10^3 for about 1 year, but this memory required 100 V to switch over a period of 1 s, and could only be switched for 50 cycles. In comparison, flash memory exhibits write speeds of 1 μs, retention times of 10 years, and can be cycled at least 10^4 times.[23]

(Received January 25, 2017; accepted March 7, 2017; published online March 27, 2017)

A third approach to making a printable memory is to utilize materials that exhibit resistive switching; devices based on this mechanism are often referred to as memristors.[24] Typical memristors consist of a solid electrolyte between two metal electrodes, and are made using vapor-phase methods that allow for the creation of a very thin (30–50 nm) solid electrolyte layer.[25] Memristor devices made with vapor phase methods have exhibited write speeds as small as 0.1 ns (1000× faster than flash), up to 10^{11} switching cycles, and data retention times of up to 10 years. These performance metrics indicate that resistive switching is one of the most promising approaches to realizing a high-performance fully printed memory. To create fully printed memristor devices, the metal electrodes are typically made with silver nanoparticle (Ag NP) and copper nanoparticle (Cu NP) inks,[26] and the solid electrolytes are made from metal oxide nanoparticles such as TiO_2,[26–28] ZrO_2,[29] ZnO,[30] CuO_x,[31] and MoO_x/MoS_2.[32] Although a TiO_2-based device reported a switching speed faster than flash (250 ns), it retained information for only 3 h, and required a sintering temperature of 500°C.[28] The best retention time for a printable memristor was 11 days for a ZrO_2-based device,[29] and the best endurance was 10^4 cycles for an MoO_x/MoS_2-based device.[32] Although the endurance of 10^4 cycles is comparable to flash, the MoO_x/MoS_2-based device retained information for only a few hours, and had a switching speed of 5 ms. It may be that the poor performance of fully printed memristors relative to their vapor-phase deposited counterparts is the greater thickness (~100 nm) of the electrolyte or the roughness of the electrolyte/electrode interfaces. Table I summarizes the performance metrics for every fully printed memory that has been reported. As yet, no fully printed device has reported excellent all-around performance: write speeds below 10 μs, retention times of 10 years, and an endurance greater than or equal to 10^4 cycles.

Excellent resistive switching properties have previously been observed using a thin film loaded with copper–silica core–shell nanowires (Cu–SiO_2 NWs).[33] These devices have modest switching voltages (2 V), a fast switching speed (50 ns), good endurance ($>10^4$ cycles), and data retention times (4 days) comparable to other fully printed memristors. In this work, we utilize Cu–SiO_2 NWs to create a fully printed programmable crossbar array of nonvolatile memory devices. The crossbar array consists of 16 individual memristors with printed Au bottom contacts, a printed polymer/Cu–SiO_2 NW composite as the resistive switching layer, and printed Cu top contacts. All layers were printed with an aerosol jet. The memristors made in this way exhibited switching voltages of 3 ± 2 V, endurances of at least 10^4 cycles, 10 years of ON state retention, and write speeds of 3 ± 2 μs. These devices thus meet the performance requirements necessary for use as a fully printed memory. We demonstrate the integration of these fully printed memristor arrays into a circuit to illustrate the use of a 4-bit memory to control LEDs.

METHODS

Cu–SiO_2 NW Synthesis

Cu NWs were synthesized in a manner similar to that reported previously.[34] To start with, 50 mL of 0.1 M $Cu(NO_3)_2$ (Fischer Scientific, 99%), 7.5 mL of ethylenediamine (EDA; Fischer Scientific 99%), and 1 L of 12 M NaOH (NOAH, 99%) were added together in a 2 L round-bottom flask and agitated by hand until mixed. The solution was then heated to 50°C while stirring vigorously, 1.25 mL of hydrazine (Fischer Scientific, 98% anhydrous) was added, and the solution continued to be stirred for 5 min. The solution was then left unstirred for 90 min to allow for Cu NW growth. The Cu NW product was then rinsed in a solution of polyvinylpyrrolidone (3 wt.% PVP in H_2O; Aldrich, 10,000 MW) and 1% diethylhydroxylamine (1 wt.% DEHA in H_2O; Aldrich) using a 2 L separation funnel. The procedure was repeated until the Cu NWs were dispersed in solution. After rinsing, the Cu NWs were dispersed in 1 L of the 3 wt.% PVP and 1 wt.% DEHA solution. The solution concentration was analyzed via atomic absorption spectroscopy using a Perkin Elmer 3100 spectrophotometer. The concentration of Cu NWs in the final storage solution was 4.5 mg/mL.

The Cu NWs were coated with SiO_2 using a modified Stöber reaction that was originally developed for coating Ag NPs,[35] but which we modified for coating SiO_2 on Cu NWs. To start, 15.34 mg (3.41 mL of the storage solution) of Cu NWs were dispersed into 1.7 mL of an aqueous solution containing 1% PVP (10,000 MW). The solution was added to 10.5 mL of ethanol (EtOH, 190 proof; Koptec), and stirred at 300 rpm in a 20 mL scintillation vial. Subsequently, 282 μL of dimethylamine solution (40 wt.% DMA in H_2O; Aldrich) and 40 μL of tetraethylorthosilicate (TEOS, 98%; Acros Organics) were added. The reaction was left to stir for 10 min under ambient conditions. The reaction solution was then added to a 50 mL centrifuge tube containing 36 mL of 40:60 EtOH:H_2O to dilute to a 50:50 mixture of EtOH:H_2O. This solution was centrifuged at 2000 rpm for 10 min. The supernatant was removed, and the wires were rinsed three times with methanol (MeOH, 200 proof; Koptec) using the same centrifugation parameters. The solution was then concentrated to 10 mL in MeOH. A 5 μL portion was dried on ultrathin carbon supported by lacey carbon on a 400-mesh copper grid for transmission electron microscopy with a FEI Tecnai G^2 Twin Transmission Electron Microscope.

Table I. Comparison of previously published fully printed memories and this current work (in bold)

Materials (electrode/switching layer/electrode)	Memory type	Write speed	Write/erase voltages	Data retention time	ON/OFF cycling endurance
Ag/TiO_2/C[27]	Resistive	100 μs	2 V/−3 V	8 h	10^3 cycles
Ag/TiO_2/Mo–In_2O_3[28]	Resistive	250 ns	3 V/−3 V	3 h	10^3 cycles
Ag/MoO_x–MoS_2/Ag[32]	Resistive	5 ms	1.5 V/−1.5 V	3 h	10^4 cycles
PEDOT:PSS/PMMA–rGO/PEDOT:PSS[19]	Charge-trap	1 s	100 V/−100 V	1 year	50 cycles
Ag/ZrO_2/Ag[46]	Resistive	–	3 V/−3 V	–	140 cycles
Ag/ZrO_2/Ag[29]	Resistive	–	3 V/−3 V	11 days	50 cycles
Ag/TiO_2/Cu[26]	Resistive	–	0.7 V/−0.7 V	–	–
Ag/TiO_2/Ag[47]	Resistive	5 ms	1.5 V/−1.5 V	–	–
Ag/TiO_2/Ag[48]	Resistive	–	1 V/−0.5 V	–	100 cycles
Ag/ZnO/Cu[30]	Resistive	–	1.3 V/−1.3 V	–	500 cycles
Ag/AgO–CuO/Cu[49]	Resistive	–	2 V/−3 V	–	40 cycles
Ag/CuO_x/Cu[31]	Resistive	–	1 V/−1 V	2 weeks	100 cycles
Ag/$ZnSnO_3$/Ag[50]	Resistive	–	2 V/−2 V	24 min	100 cycles
Ag/$ZnSnO_3$–PVA/Ag[21]	Charge-trap	–	1.5 V/−1.5 V	36 h	500 cycles
ITO/GaZnO/ITO[51]	Charge-trap	–	6 V/−7 V	–	300 cycles
PEDOT:PSS/polyvinylphenol/PEDOT:PSS[52]	Charge-trap	–	30 V/−20 V	–	100 cycles
Ag/MoS_2–PVA/Ag[22]	Charge-trap	–	3 V/−3 V	1 day	10^3 cycles
Au/Cu–SiO_2/Cu (this work)	**Resistive**	**3 μs**	**3 V/−3 V**	**10 years**	**10^4 cycles**

Device Manufacturing

Au electrodes were printed using an Au ink (UTD-Au40; UT Dots) containing 40 wt.% Au nanoparticles. The ink was printed as received on glass slides or polyimide film by an AJ-300 aerosol jet printer (Optomec, USA). A 150 μm-diameter nozzle was used for printing, and the flow rates of sheath gas and carrier gas were set to 50 sccm, and 20 sccm, respectively. The platen temperature was maintained at 60°C, and the printed Au nanoparticle layers were further sintered at 280°C in air for 1 h in an oven. The printed film thickness was 450 nm, and the sheet resistance was 1.5 Ω/sq.

Cu–SiO_2 NWs in MeOH were rinsed into a 30-mL solution of 1.5 wt.% ethylcellulose (Ethocel 10; Dow) in MeOH. To facilitate the aerosol jet printing of the ink, 10% α-terpineol (≥96%; Aldrich) was added as a cosolvent into the ink to adjust its viscosity and evaporation rate. The as-prepared Cu-SiO_2 NW ink was printed using a wide nozzle with a diameter of 1 mm, and the sheath, carrier and exhaust gas flow rates were set to be 60 sccm, 500 sccm, and 480 sccm, respectively. All printing was carried out in air at room temperature while the platen was maintained at 70°C to accelerate ink drying. The printed film thickness is around 4.5 μm.

Cu NP metal–organic decomposition (MOD) ink was made using a modified procedure reported by Shin et al.[36] To start, 10 mL of MeOH, 40 mmol of 2-amino-2-methyl-1-propanol (AMP, >99%, Aldrich), and 40 mmol of octylamine (99%, Alfa Aesar) was stirred for 30 min. Next, 40 mmol of copper(II) formate tetrahydrate (98%; Santa Cruz Biotechnology) was added, and stirred for 1 h. The subsequent solution was placed in a vacuum oven for 12 h under reduced pressure at 50°C to remove MeOH. The ink was completed by mixing the vacuumed product in a 3:2 weight ratio with isopropyl alcohol (IPA, 99.5%; BDH). The ink was printed on top of the Cu–SiO_2 layer using the AJ-300 printer. A 150 μm diameter nozzle was used for printing, and the flow rates of sheath gas and carrier gas were set to 40 sccm and 25 sccm, respectively. The platen temperature was set to 40°C during printing. The printed samples were reduced and sintered at 160°C for 30 min in a tube furnace under a flow of N_2. The printed film thickness was 900 nm.

Switching Measurements

Switching tests were performed with a Keithley 2400 SourceMeter connected via copper clips to the printed Au and Cu electrodes. The switching programs were written in LabVIEW 2012. Switching cycles were performed using a voltage sweep with a compliance current of 100 μA. Sweeps were performed at a rate of 1.5 V/s. Write and erase voltages are logged by reading the voltage recorded immediately before the switch occurs, and the ON and OFF resistances were recorded by reading the resistance after each sweep at a read voltage of 100 mV.

Write Speed Measurements

Write speed tests were performed using an Arduino UNO in conjunction with a VOLTEQ power supply, with voltages read using a Hantek DSO 5200A Oscilloscope. A schematic of the switching speed measurement is provided in Fig. S1. A 150 kΩ resistor is in line with the memristor to limit the current through the memristor, and the voltage

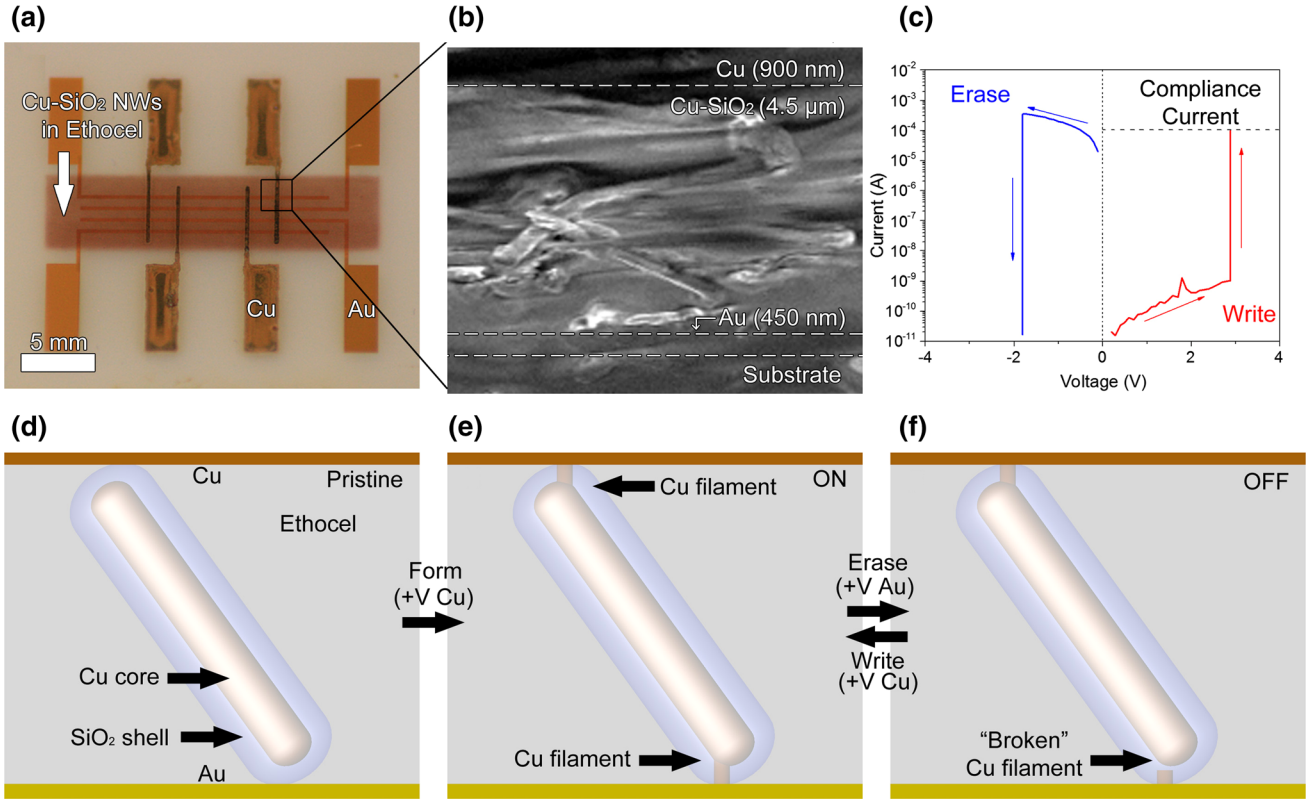

Fig. 1. (a) Fully printed and sintered device with (b) SEM image of a cross-section of the polymer/NW composite film. (c) Plot of the current and voltage in the memristor during erasing and writing. (d) Cross-sectional schematics illustrating the operating mechanism of the memristor. Application of a positive bias to the Cu top contact induces the growth of Cu filaments to form a conductive pathway, resulting in the (e) ON state. The memristor can then be erased by applying a reverse bias to dissolve the filament, resulting in (f) the OFF state.

across this resistor is measured to calculate the current through the memristor. A 6 MΩ resistor is placed after the 1.5 kΩ counter-resistor to measure the maximum voltage from the output pulse. Confirmation of the ON state was obtained by using the Keithley 2400 to measure the resistance of the memristor before and after pulse application. The maximum voltage of the instrument (~10 V) was applied in order to minimize write speed.[37]

Programming Tests

Programming tests were performed with an Arduino UNO, Keithley 2400 SourceMeter, and VOLTEQ power supply. A 4-bit array of memristors was programmed by supplying a 5 V pulse for 500 ms using four outputs from the Arduino. An 8.1 kΩ resistor was placed in line of each memristor to limit the current through the memristors. A 56-kΩ resistor was also added between the base of each transistor and ground. The memristors were read by supplying 0.7 V across all four memristors using a Keithley 2400 SourceMeter. In the OFF state, 0.7 V is insufficient to turn on the npn bipolar junction transistors (BJT) due to the voltage drop across the memristor. In the ON state, the voltage drop over the memristor is low, allowing the 0.7 V bias to turn on the BJT and thereby light the LED. Erasing of the device was performed using the previously described LabVIEW program to sweep negative voltage across each memristor until the device was completely erased.

RESULTS AND DISCUSSION

Device Imaging

Figure 1a shows the final crossbar array consisting of 16 individual memristors on glass. Figure 1b displays an SEM image of a cross-section of one of the memristors, showing the nanowires embedded within the composite switching layer. TEM images (Fig. S2) show an example of the SiO_2 shells grown on the copper nanowires. The average thickness of the SiO_2 shells was 18 ± 3.6 nm, which is thin enough to allow for consistent resistive switching,[37] but thick enough to electrically insulate the nanowires from one another.[33]

Resistive Switching

After printing the array, an initial forming step enables its use as a memristor. A characteristic *I–V* curve for the forming step is shown in Fig. S3. As

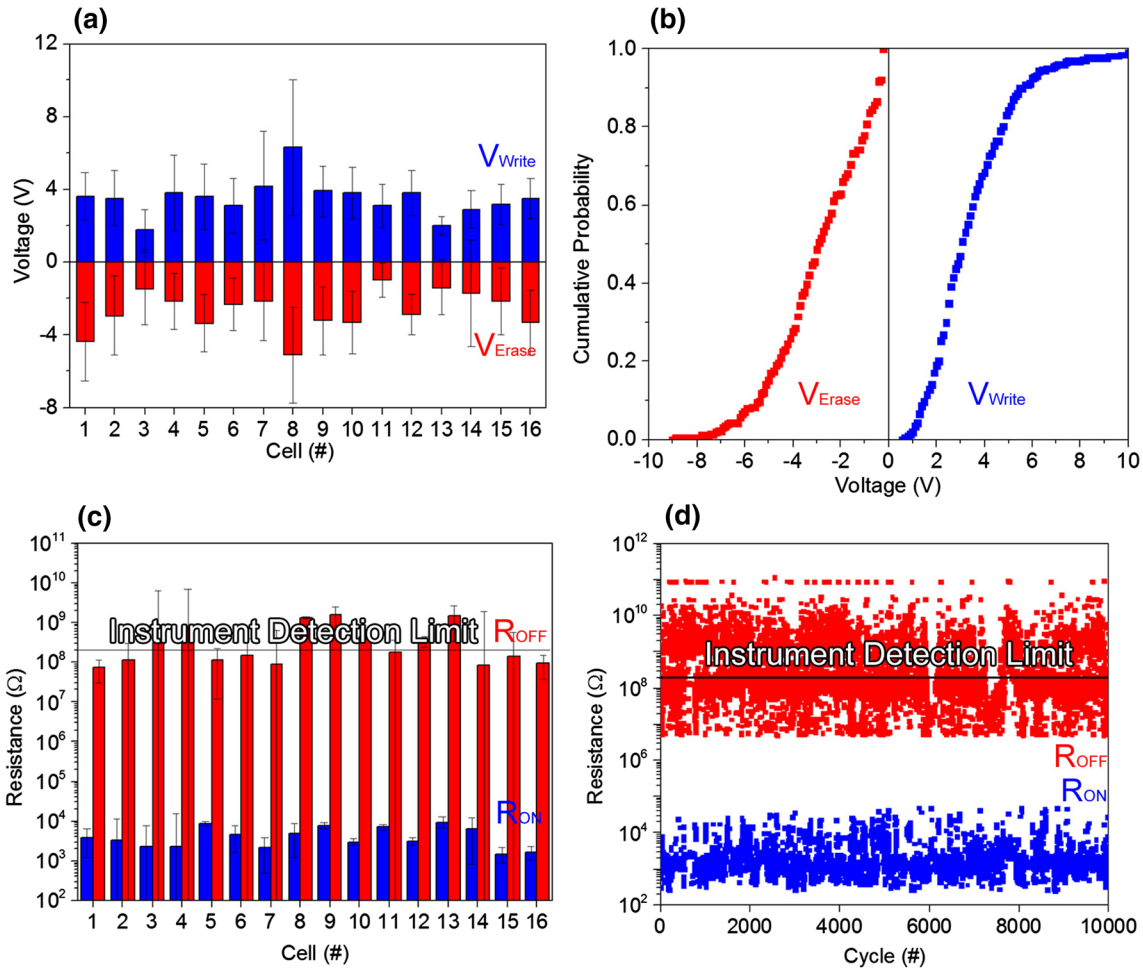

Fig. 2. (a) Average write and erase voltages (n = 20) for each memristor of the 16-memristor crossbar. (b) Cumulative probability of write and erase voltages (n = 320) over all memristors. (c) Average ON and OFF resistances (n = 20) in each memristor of the 16-memristor crossbar. (d) ON and OFF resistances over 10^4 switching cycles show no degradation in performance. The horizontal lines labeled instrument detection limit indicate the highest resistance that can be accurately measured given a 100-mV read voltage with the instrument used.

the voltage applied to the Cu top contact is swept in the positive direction, the current increases by 100,000 times at 9 V, and is limited by a compliance current set to 100 μA. After the forming step, the device can be reversibly switched between a low-resistance and high-resistance state. Figure 1c shows a typical I–V curve for bipolar resistive switching of the device. After a memristor has gone through the forming stage and is in the low-resistance state, it can be turned back to the OFF state by reversing the bias, with a positive bias applied to the bottom Au contact. When the voltage reaches −3 V, the current decreases by 100,000 times as the memory reverts to the high-resistance state. The memristor can again be returned to the low-resistance ON state by application of a positive bias to the Cu top contact.

It is thought that the resistance of the SiO_2 junctions between the nanowires and the contacts drops due to an electrochemical metallization

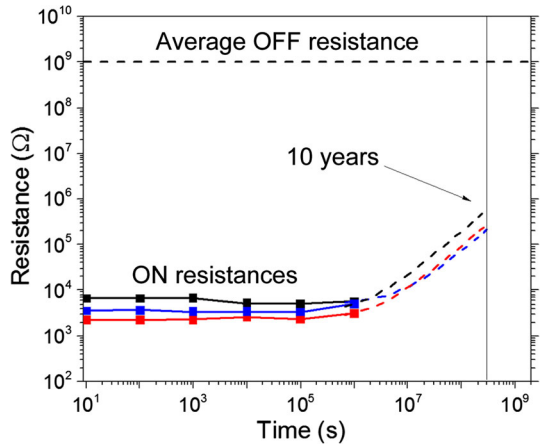

Fig. 3. ON resistances versus time shows the memristor retains its ON state for at least 10^6 s over three separate devices. A linear extrapolation of the data (dotted lines) suggests that the device will retain the ON state for at least 10 years.

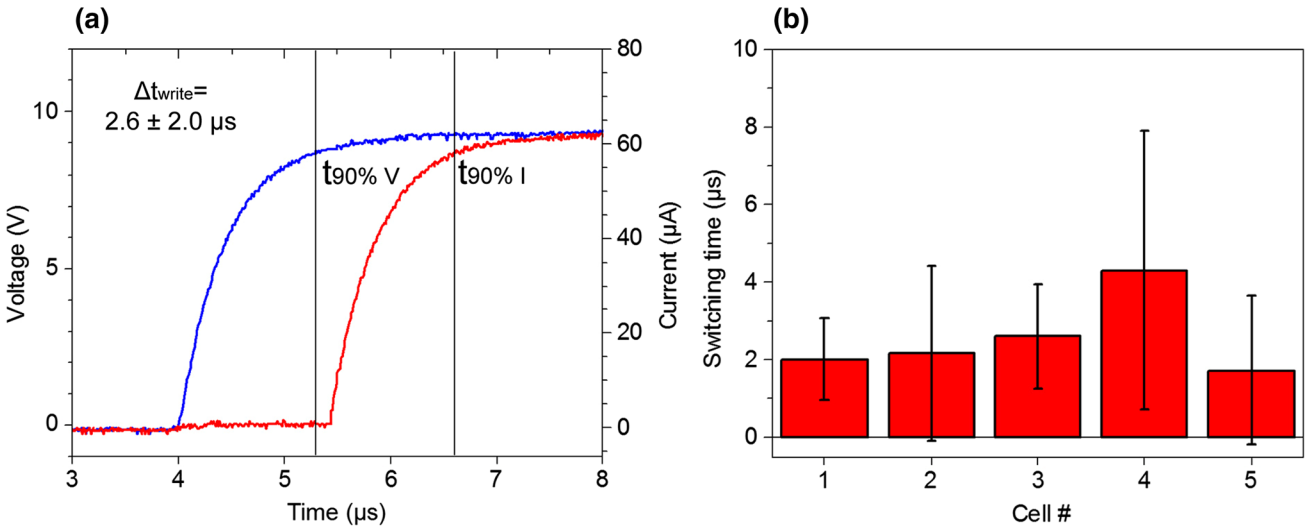

Fig. 4. (a) Write speed characteristics of a single write step. The delay between the applied voltage and the current response at 90% of the maximum amplitude was used to determine the write time. (b) Averages and standard deviations of switching speeds ($n = 5$) in five different memristors.

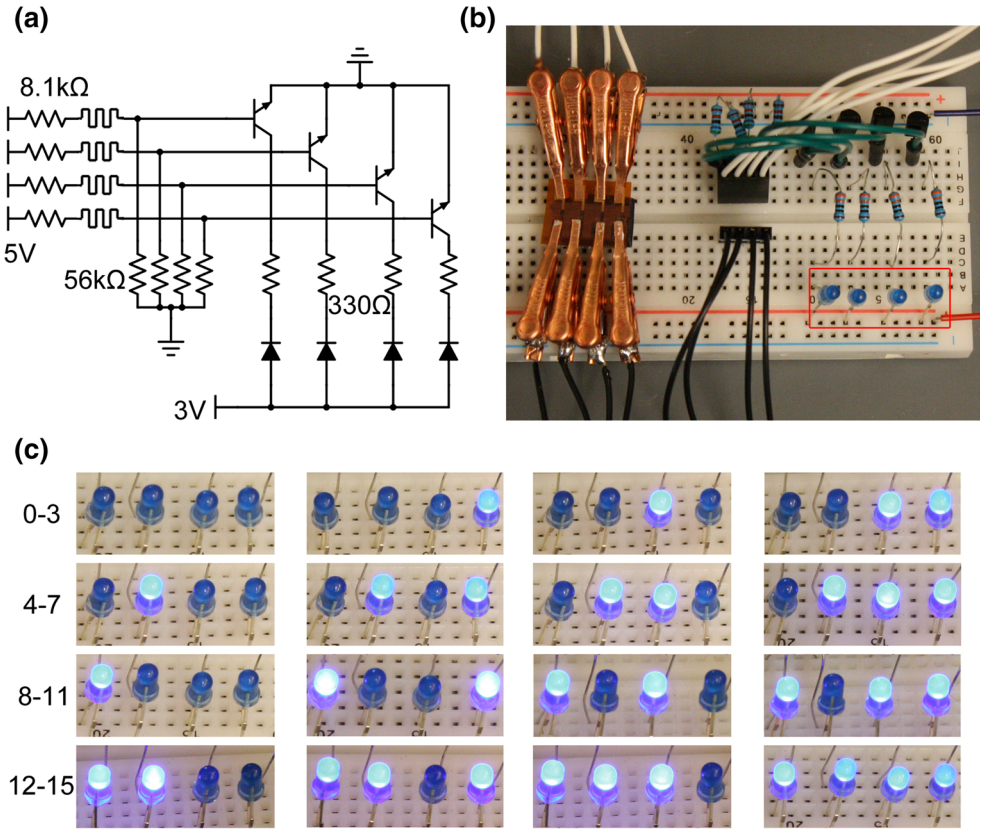

Fig. 5. Example circuit utilizing a 4-bit fully printed memristor. (a) A circuit diagram and (b) the programming circuit. LEDs are highlighted in red. (c) LEDs illustrating the programmed states of the 4-bit memristor. Numbers indicate the binary numbers programmed in each row (Color figure online).

mechanism, in which the positive bias results in dissolution of the Cu top contact, diffusion of Cu ions through the SiO_2 shell, and reduction of Cu ions on a Cu NW until a Cu filament forms between the Cu NW and the top contact (Fig. 1d and e).[25,33] Filament formation subsequently takes place in a similar manner between the Cu NW and the Au bottom contact, resulting in a dramatic drop in the

resistance between the top and bottom contacts. This low-resistance state is the ON state. To switch the device back to the OFF state, a negative bias can be applied to the Cu electrode, resulting in anodic dissolution of the Cu filament in the SiO_2 shell between the Cu NW and the Au electrode (Fig. 1f). In the OFF state, the device can be switched back ON by reapplication of a positive bias to the Cu electrode, leading to regrowth of the filament. Because of the shorter distance Cu ions migrate for the write step compared to the form step, the voltage required for writing (3 V) is less than that required for forming (9 V).[38]

Figure 2a shows the average and standard deviation of the switching voltages for every memristor in the 16-memristor crossbar device. Each memristor was cycled multiple times, and each exhibited moderate operating voltages, with average writing voltages ranging from 1.8 V to 6.3 V, and average erasing voltages between −1.0 V and −5.1 V. Figure 2b shows the cumulative switching voltages, summing the 20 cycles over all 16 memristors (n = 320). The average write voltage across all memristors was 3.4 V, with a maximum of 10 V. The average erase voltage was −2.8 V, with a maximum −9.0 V.

Figure 2c shows the average ON and OFF resistances of each memristor. The average ON resistance across all 16 memristors was 4.4 kΩ, with the individual average ON resistances ranging between 1.5 kΩ and 9.4 kΩ. Across all 16 memristors, the average OFF resistance was above the instrument detection limit of 200 MΩ. The lowest average OFF resistance measured for a single memristor was 73 MΩ, resulting in a minimum R_{OFF}/R_{ON} of 10^4. Figure 2d shows that the memristor is capable of switching with $R_{OFF}/R_{ON} > 10^5$ over 10^4 cycles with no observable degradation. The OFF state appears noisy due to the limit of detection of the instrument at high resistance values. We stopped testing at 10^4 cycles due to time limitations (one such test takes 10 days), but given the lack of degradation, it appears the endurance may be higher than 10^4 cycles.

Three devices were tested for retention of the ON state over time in air at room temperature (Fig. 3). Over three different memristors, the ON state was read periodically with a 100 mV read voltage over the course of 10^6 s. The memristors retained the ON state and showed negligible degradation over this period. Linearly extrapolating the data out to 10 years (a method that has been previously employed to estimate retention times[39,40]) shows that the ON state resistance will remain at least 10^3 times lower than the OFF state resistance. This is a significant improvement over the retention time of 4 days observed previously,[33] and may be due to the presence of the ethylcellulose reducing the diffusion of air into the resistive switching layer.

The write speed of the system was characterized by applying a 10 V write voltage across a memristor, and measuring the time delay between when 90% of the maximum write voltage is applied and when 90% of the maximum response current is read (Fig. 4a). The response current indicates when the memristor has entered the ON state; the delay between when the write voltage is applied and when the memristor is ON indicates the time it takes to write to the memristor. By measuring five replicates across five different memristors (n = 25), the average write speed was determined to be 3 μs (Fig. 4b). This write speed is faster than all but one previously reported fully printed memory, and is comparable to the write speed of flash memories.

Circuit Integration

To illustrate how these fully printed memristors might be used in an application, we integrated them into a circuit that allowed their ON state to be visualized with an LED. Instead of the crossbar array, we used a set of four memristors in parallel to act as a 4-bit memory. We did not use the crossbar array because of the presence of sneak paths, which is a known issue for memristors fabricated in such a geometry.[41–45] The ability to write or read a memristor in a high-resistance state can be inhibited by neighboring memristors in low-resistance states which allow the current to flow around the high-resistance memristor. This leads to reading and writing errors. Figure 5a illustrates the circuit diagram used to program the 4-bit memory, and Fig. 5b shows a photograph of the programming circuit connected to the device. All 16 programming states of the 4-bit memory are shown in binary in Fig. 5c. These states were set with a 5.0 V write voltage from an Arduino, and read with 0.7 V in parallel across all the memristors. In the ON state, the memristor allows the 0.7 V bias to turn on the gate of a transistor, which in turn turns on an LED. While simple, this example of lighting LEDs illustrates successful programming and ON state retention in an actual circuit. A more practical use might be to send the 4-bit output to a BCD-to-7-segment display driver, which in turn could control a 7-segment LED to communicate the price of an item on a shelf. Alternatively, the 4-bit output could be fed to a 4-to-16 multiplexer for a multitude of applications.

CONCLUSIONS

In summary, a fully printed array of memristors has been manufactured with excellent overall performance metrics: endurance of $>10^4$ cycles, a retention time >10 years, and write speeds of 3 μs. No previous fully printed memory has exhibited such a combination of excellent performance characteristics. The memory can be easily written with 5 V and read with 0.7 V, making it compatible with standard microcontrollers. Future work might explore the integration of fully printed diodes into the crossbar architecture to eliminate sneak paths,

or interfacing with fully printed transistors to enable the addressing of larger memory arrays.

ACKNOWLEDGEMENTS

This work was supported by an NSF CAREER award (Grant DMR-1253534). MJC acknowledges support through the SMIF Voucher Program.

ELECTRONIC SUPPLEMENTARY MATERIAL

The online version of this article (doi: 10.1007/s11664-017-5445-5) contains supplementary material, which is available to authorized users.

REFERENCES

1. K. Suganuma, *Introduction to Printed Electronics* (New York: Springer, 2013).
2. T.H. Van Osch, J. Perelaer, A.W. de Laat, and U.S. Schubert, *Adv. Mater.* 20, 343 (2008).
3. P.H. Lau, K. Takei, C. Wang, Y. Ju, J. Kim, Z. Yu, T. Takahashi, G. Cho, and A. Javey, *Nano Lett.* 13, 3864 (2013).
4. F. Molina-Lopez, D. Briand, and N.F. de Rooij, *Sens. Actuator B Chem.* 166, 212 (2012).
5. L. Yang, A. Rida, R. Vyas, and M.M. Tentzeris, *IEEE Trans. Microwave Theory Tech.* 55, 2894 (2007).
6. A. Facchetti, *Chem. Mater.* 23, 733 (2010).
7. P. Kopola, M. Tuomikoski, R. Suhonen, and A. Maaninen, *Thin Solid Films* 517, 5757 (2009).
8. A.R. Rathmell, S.M. Bergin, Y.L. Hua, Z.Y. Li, and B.J. Wiley, *Adv. Mater.* 22, 3558 (2010).
9. J. Lee, P. Lee, H.B. Lee, S. Hong, I. Lee, J. Yeo, S.S. Lee, T.-S. Kim, D. Lee, and S.H. Ko, *Adv. Funct. Mater.* 23, 4171 (2013).
10. J. Chang, X. Zhang, T. Ge, and J. Zhou, *Org. Electron.* 15, 701 (2014).
11. A.M. Gaikwad, D.A. Steingart, T.N. Ng, D.E. Schwartz, and G.L. Whiting, *Appl. Phys. Lett.* 102, 233302 (2013).
12. A.C. Arias, J. Daniel, B. Krusor, S. Ready, V. Sholin, and R. Street, *J. Soc. Inf. Disp.* 15, 485 (2007).
13. M. Magliulo, M. Mulla, M. Singh, E. Macchia, A. Tiwari, L. Torsi, and K. Manoli, *J. Mater. Chem. C* 3, 12347 (2015).
14. S.-T. Han, Y. Zhou, and V.A.L. Roy, *Adv. Mater.* 25, 5425 (2013).
15. H.-T. Lin, Z. Pei, J.-R. Chen, C.-P. Kung, Y.-C. Lin, C.-M. Tseng, and Y.-J. Chan, in *2007 IEEE International Electron Devices Meeting* (IEEE, 2007), pp. 233–236.
16. U.S. Bhansali, M.A. Khan, and H.N. Alshareef, *Microelectron. Eng.* 105, 68 (2013).
17. T.N. Ng, D.E. Schwartz, L.L. Lavery, G.L. Whiting, B. Russo, B. Krusor, J. Veres, P. Bröms, L. Herlogsson, N. Alam, O. Hagel, J. Nilsson, and C. Karlsson, *Sci. Rep.* 2, 585 (2012).
18. J.Y. Bak, S.W. Jung, and S.M. Yoon, *Org. Electron.* 14, 2148 (2013).
19. C. Kim, J.-M. Song, J.-S. Lee, and M.J. Lee, *Nanotechnology* 25, 014016 (2013).
20. K.J. Baeg, D. Khim, J. Kim, B.D. Yang, M. Kang, S.W. Jung, I.K. You, D.Y. Kim, and Y.Y. Noh, *Adv. Funct. Mater.* 22, 2915 (2012).
21. G.U. Siddiqui, M.M. Rehman, and K.H. Choi, *Polymer* 100, 102 (2016).
22. M.M. Rehman, G.U. Siddiqui, J.Z. Gul, S.-W. Kim, J.H. Lim, and K.H. Choi, *Sci. Rep.* 6, 36195 (2016).
23. P.A. Laplante and S.J. Ovaska, *Real-Time Systems Design and Analysis: Tools for the Practitioner* (Hoboken: Wiley, 2011).
24. L.O. Chua, *IEEE Trans. Circuit Theory* 18, 507 (1971).
25. R. Waser, R. Dittmann, G. Staikov, and K. Szot, *Adv. Mater.* 21, 2632 (2009).
26. N. Duraisamy, N.M. Muhammad, H.-C. Kim, J.-D. Jo, and K.-H. Choi, *Thin Solid Films* 520, 5070 (2012).
27. D.-H. Lien, Z.-K. Kao, T.-H. Huang, Y.-C. Liao, S.-C. Lee, and J.-H. He, *ACS Nano* 8, 7613 (2014).
28. S.K. Vishwanath and J. Kim, *J. Mater. Chem. C* 4, 10967 (2016).
29. M.N. Awais, N.M. Muhammad, D. Navaneethan, H.C. Kim, J. Jo, and K.H. Choi, *Microelectron. Eng.* 103, 167 (2013).
30. N.M. Muhammad, N. Duraisamy, K. Rahman, H.W. Dang, J. Jo, and K.H. Choi, *Curr. Appl. Phys.* 13, 90 (2013).
31. S. Zou and C. Michael, in *2014 IEEE 64th Electronic Components and Technology Conference (ECTC)* (IEEE, 2014), pp. 441–446.
32. A.A. Bessonov, M.N. Kirikova, D.I. Petukhov, M. Allen, T. Ryhänen, and M.J. Bailey, *Nat. Mater.* 14, 199 (2015).
33. P.F. Flowers, M.J. Catenacci, and B.J. Wiley, *Nanoscale Horiz.* 1, 313 (2016).
34. S. Ye, A.R. Rathmell, Y.-C. Ha, A.R. Wilson, and B.J. Wiley, *Small* 10, 1771 (2014).
35. Y. Kobayashi, H. Katakami, E. Mine, D. Nagao, M. Konno, and L.M. Liz-Marzán, *J. Colloid Interface Sci.* 283, 392 (2005).
36. D.-H. Shin, S. Woo, H. Yem, M. Cha, S. Cho, M. Kang, S. Jeong, Y. Kim, K. Kang, and Y. Piao, *ACS Appl. Mater. Interfaces* 6, 3312 (2014).
37. C. Schindler, M. Weides, M.N. Kozicki, and R. Waser, *Appl. Phys. Lett.* 92, 122910 (2008).
38. C. Schindler, G. Staikov, and R. Waser, *Appl. Phys. Lett.* 94, 072109 (2009).
39. S. Kim, H. Moon, D. Gupta, S. Yoo, and Y.K. Choi, *IEEE Trans. Electron. Devices* 56, 696 (2009).
40. J.W. Seo, J.-W. Park, K.S. Lim, S.J. Kang, Y.H. Hong, J.H. Yang, L. Fang, G.Y. Sung, and H.-K. Kim, *Appl. Phys. Lett.* 95, 133508 (2009).
41. E. Linn, R. Rosezin, C. Kugeler, and R. Waser, *Nat. Mater.* 9, 403 (2010).
42. K.-H. Kim, S. Gaba, D. Wheeler, J.M. Cruz-Albrecht, T. Hussain, N. Srinivasa, and W. Lu, *Nano Lett.* 12, 389 (2012).
43. M.A. Zidan, H.A.H. Fahmy, M.M. Hussain, and K.N. Salama, *Microelectron. J.* 44, 176 (2013).
44. J.J. Yang, M.-X. Zhang, M.D. Pickett, F. Miao, J.P. Strachan, W.-D. Li, W. Yi, D.A. Ohlberg, B.J. Choi, and W. Wu, *Appl. Phys. Lett.* 100, 113501 (2012).
45. J. Zhou, K.-H. Kim, and W. Lu, *IEEE Trans. Electron. Devices* 61, 1369 (2014).
46. M.N. Awais, H.C. Kim, Y.H. Doh, and K.H. Choi, *Thin Solid Films* 536, 308 (2013).
47. P. Vilmi, M. Nelo, J.-V. Voutilainen, J. Palosaari, J. Pörhönen, S. Tuukkanen, H. Jantunen, J. Juuti, and T. Fabritius, *Flex. Print. Electron.* 1, 025002 (2016).
48. K. Rahman, M. Mustafa, N. Muhammad, and K. Choi, *Electron. Lett.* 48, 1261 (2012).
49. S. Zou, P. Xu, and M. Hamilton, *Electron. Lett.* 49, 829 (2013).
50. G. Siddiqui, J. Ali, Y.-H. Doh, and K.H. Choi, *Mater. Lett.* 166, 311 (2016).
51. A. Kim, K. Song, Y. Kim, and J. Moon, *ACS Appl. Mater. Interfaces* 3, 4525 (2011).
52. M.N. Awais and K.H. Choi, *Electron. Mater. Lett.* 10, 601 (2014).